(12) LEVEL II

NRL Report 8421

Bearing-Only Tracking Algorithms

ALEX GRINDLAY

Radar Analysis Branch
Radar Division

July 16, 1980

NAVAL RESEARCH LABORATORY
Washington, D.C.

SECURITY CLASSIFICATION OF THIS PAGE (When Data Entered)

12 18

REPORT DOCUMENTATION PAGE

READ INSTRUCTIONS BEFORE COMPLETING FORM

1. REPORT NUMBER: NRL Report 8421
2. GOVT ACCESSION NO.: AD-A088093
3. RECIPIENT'S CATALOG NUMBER:

4. TITLE (and Subtitle): BEARING-ONLY TRACKING ALGORITHMS
5. TYPE OF REPORT & PERIOD COVERED: Final report on one phase of a continuing NRL problem
6. PERFORMING ORG. REPORT NUMBER:

7. AUTHOR(s): Alex Grindlay
8. CONTRACT OR GRANT NUMBER(s): F12151

9. PERFORMING ORGANIZATION NAME AND ADDRESS: Naval Research Laboratory, Washington, DC 20375
10. PROGRAM ELEMENT, PROJECT, TASK AREA & WORK UNIT NUMBERS: NRL Problem 53-0612-0-0, Program Element 62712N, Project ZF12 151 701

11. CONTROLLING OFFICE NAME AND ADDRESS: Department of Navy, Chief of Naval Material, Washington, DC 20360
12. REPORT DATE: July 16, 1980
13. NUMBER OF PAGES: 18

14. MONITORING AGENCY NAME & ADDRESS (if different from Controlling Office): NRL-8421
15. SECURITY CLASS. (of this report): UNCLASSIFIED
15a. DECLASSIFICATION/DOWNGRADING SCHEDULE:

16. DISTRIBUTION STATEMENT (of this Report)

Approved for public release; distribution unlimited.

17. DISTRIBUTION STATEMENT (of the abstract entered in Block 20, if different from Report)

DTIC ELECTE AUG 19 1980 S D B

18. SUPPLEMENTARY NOTES

19. KEY WORDS (Continue on reverse side if necessary and identify by block number)

Tracking algorithms
Kalman filter
Triangulation

20. ABSTRACT (Continue on reverse side if necessary and identify by block number)

The problem of tracking emitters, via asynchronous bearing measurements made at two remote sites, was addressed. Three algorithms were developed for this purpose: a statistical moving average technique, a modified Kalman filter technique, and an extended Kalman filter technique. The performances of the algorithms in several selected scenarios were com ed, with the preliminary results indicating that the modified Kalman filter technique is superior in its ability to rapidly develop a reasonable track. The extended Kalman filter technique demonstrated superior tracking performance

(Continues)

DD FORM 1 JAN 73 1473 EDITION OF 1 NOV 65 IS OBSOLETE
S/N 0102-014-6601

SECURITY CLASSIFICATION OF THIS PAGE (When Data Entered)

251950

20. Abstract (Continued)

once it had settled down; however, for the cases considered this required an unreasonable amount of time. Further investigation is required to assess the performance of the algorithms against maneuvering targets. The effect of varying the time between measurements should also be considered.

CONTENTS

BEARING-ONLY TRACKING ALGORITHMS

INTRODUCTION

A number of studies in locating electronic emitters have been conducted, and algorithms (given in papers such as Refs. 1, 2, and 3) have been developed which provide estimates of emitter locations based on bearing measurements. For the most part, these algorithms are concerned with the problem of locating stationary emitters, or relatively slow moving emitters, based on measurements made by a single moving platform. We will modify two of these algorithms such that a moving emitter's location can be estimated by using bearing measurements from two stationary sites. This was accomplished by thinking of the stationary sites as a single platform which was moving rapidly back and forth between the sites. A third algorithm, the modified Kalman filter technique, was also developed. This technique also uses bearing measurements from two sites to estimate the emitter's location but is not dependent on the technology developed for locating emitters from a single moving platform. All methods involve some form of triangulation.

The performances of the three algorithms were compared by operating them in identical scenarios using a computer simulation. Emitter motion was restricted to constant-velocity straight-line motion. Random errors were introduced to the measurements by selecting samples from a normal noise distribution derived from a random-number generator. A standard deviation of 1° was assumed for the angular-bearing noise distribution. Bearing measurements were made every 2 s from alternate sites.

STATISTICAL MOVING AVERAGE TECHNIQUE

The first technique to be considered was developed from an algorithm presented in Ref. 1. In its original form the algorithm was used by a moving platform to estimate the position of a stationary emitter. It was also demonstrated that the algorithm could be used to detect emitter motion. However, no attempt was made by the authors of Ref. 1 to use the algorithm in a tracking mode, since it provided erratic location estimates when the speed of the emitter was of the same order as that of the platform.

If one considers the case of two sites that are sharing bearing information on a single emitter, one can think of the sites as a single platform which is moving rapidly back and forth between the sites. This leads to the following adaptations of the algorithm. In Fig. 1 we have two detecting sites at (x_1, y_1) and (x_2, y_2). Without loss of generality the sites have been located on the x axis. An emitter is at (x, y), and the current best estimate of its position is $(\hat{x}, \hat{y})$. The angle H corresponds to the heading in the single moving platform case [1] and is measured clockwise from north. The bearing angle B_i is measured clockwise from the baseline, and the angle $(H + B_i)$ is measured clockwise from north. The true, measured, and estimated bearings are given by B_i, $\tilde{B}_i$, and $\hat{B}_i$ respectively, with the subscript i being incremented each time a site makes a measurement. The error in the bearing measurement is denoted by ΔB_i, that is, $\tilde{B}_i = B_i + \Delta B_i$, and ΔB_i is assumed to be normally distributed with zero mean. The difference between the estimated position of the emitter $(\hat{x}, \hat{y})$ and the true position (x, y) is denoted by $(\Delta x, \Delta y)$:

Manuscript submitted April 13, 1980.

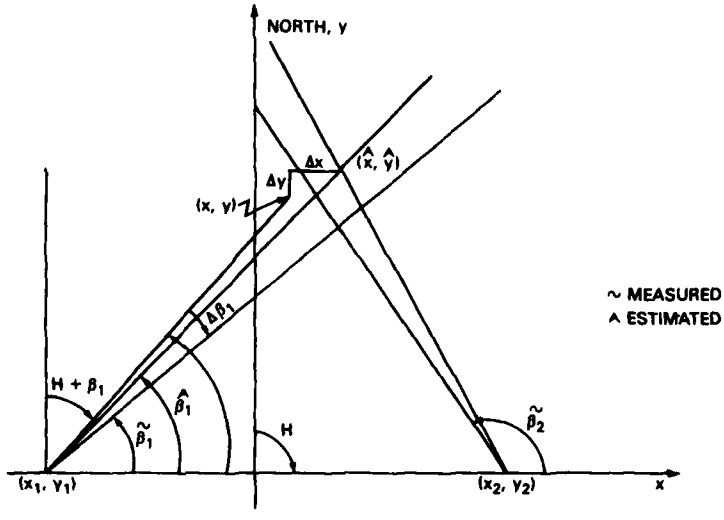

Fig. 1 — Geometry and nomenclature for the statistical moving average technique

$$\Delta x = \hat{x} - x, \tag{1}$$

and

$$\Delta y = \hat{y} - y. \tag{2}$$

To further simplify the procedure, the following notation is adopted:

$$m_i = y - y_j, \quad \hat{m}_i = \hat{y} - y_j, \tag{3}$$

$$n_i = x - x_j, \quad \hat{n}_i = \hat{x} - x_j, \tag{4}$$

where j is the site number of the site making the ith measurement. From Fig. 1

$$\cos (H + B_i) = \frac{m_i}{\sqrt{m_i^2 + n_i^2}} \tag{5}$$

and

$$\cos (H + \hat{B}_i) = \frac{\hat{m}_i}{\sqrt{\hat{m}_i^2 + \hat{n}_i^2}}. \tag{6}$$

Solving (5) and (6) for B_i and $\hat{B}_i$ yields

$$B_i = -H + \cos^{-1}\left(m_i \Big/ \sqrt{m_i^2 + n_i^2}\right) \tag{7}$$

and

$$\hat{B}_i = -H + \cos^{-1}\left(\hat{m}_i \Big/ \sqrt{\hat{m}_i^2 + \hat{n}_i^2}\right). \tag{8}$$

Making the substitutions

$$\begin{aligned} B_i &= \tilde{B}_i - \Delta B_i , \\ x &= \hat{x} - \Delta x , \\ y &= \hat{y} - \Delta y \end{aligned} \tag{9}$$

in (7) gives

$$\tilde{B} - \Delta B_i = -H + \cos^{-1}\left[\frac{\hat{m}_i - \Delta y}{\sqrt{(\hat{m}_i - \Delta y)^2 + (\hat{n}_i - \Delta x)^2}}\right]. \tag{10}$$

The quantity $(\tilde{B} - \Delta B_i)$ can be considered as a function $F_i(\Delta x, \Delta y)$ that can be expanded in a Taylor's series about the point (0, 0), giving

$$F_i(\Delta x_i, \Delta y_i) = F_i(0, 0) + \partial F_i/\partial \Delta x\Big|_{\Delta x = \Delta y = 0} \Delta x_i + \partial F_i/\partial \Delta y\Big|_{\Delta x = \Delta y = 0} \Delta y_i + \phi_i , \tag{11}$$

where ϕ_i represents higher order terms in the series. For $\Delta x = \Delta y = 0$

$$F_i(0, 0) = -H + \cos^{-1}\left(\frac{\hat{m}_i}{\sqrt{\hat{m}_i^2 + \hat{n}_i^2}}\right) = \hat{B}_i . \tag{12}$$

Making this substitution in (11) gives

$$\tilde{B} - \Delta B_i = \hat{B}_i + \partial F_i/\partial \Delta x\Big|_{\Delta x = \Delta y = 0} \Delta x_i + \partial F_i/\partial \Delta y\Big|_{\Delta x = \Delta y = 0} \Delta y + \phi_i . \tag{13}$$

Taking the partials and rearranging (13) yields

$$\tilde{B} - \hat{B}_i = \left[-\hat{m}_i(\operatorname{sgn} \hat{n}_i)/(\hat{m}_i^2 + \hat{n}_i^2)\right]\Delta x_i + \left[|\hat{n}_i|/(\hat{m}_i^2 + \hat{n}_i^2)\right]\Delta y_i + \phi_i + \Delta B_i . \tag{14}$$

Assuming that $\phi_i << \Delta B_i$, one can extend the assumption on ΔB_i to conclude that $E_i = (\phi_i + \Delta B_i)$ is normally distributed with zero mean.

The substitutions

$$Y_i = \tilde{B}_i - \hat{B}_i , \quad x_{i1} = -\hat{m}_i/(\hat{m}_i^2 + \hat{n}_i^2) , \quad \text{and} \quad x_{i2} = \hat{n}_i/\hat{m}_i^2 + \hat{n}_i^2) \tag{15}$$

gives a set of N equations for N measurements:

$$\begin{aligned} Y_1 &= X_{11}\Delta x + X_{12}\Delta y + E_1 , \\ Y_2 &= X_{21}\Delta x + X_{22}\Delta y + E_2 , \\ &\cdots \\ Y_N &= X_{N1}\Delta x + X_{N2}\Delta y + E_N . \end{aligned} \tag{16}$$

In matrix notation Eqs. (16) can be reduced to

$$Y = X\beta + E, \tag{17}$$

where

$$Y = \begin{bmatrix} Y_1 \\ Y_2 \\ \cdots \\ Y_N \end{bmatrix}, \quad X = \begin{bmatrix} X_{11} & X_{12} \\ X_{21} & X_{22} \\ \cdots & \cdots \\ X_{N1} & X_{N2} \end{bmatrix}, \quad E = \begin{bmatrix} E_1 \\ E_2 \\ \cdots \\ E_N \end{bmatrix}, \quad \text{and} \quad \beta = \begin{bmatrix} \Delta x \\ \Delta y \end{bmatrix}.$$

In Eq. (17) β and E are unknown; however, the assumption that E is normally distributed allows an estimate of β. The standard least-square estimate [4] of β is

$$\hat{\beta} = (X^T X)^{-1} X^T Y. \tag{18}$$

Starting with an initial estimate $(\hat{x}, \hat{y})$ of the emitter's position and a $(\Delta\hat{x}, \Delta\hat{y})$ as determined by Eq. (18), one can get a new estimate of the emitter's position $(\hat{\hat{x}}, \hat{\hat{y}})$:

$$\hat{\hat{x}} = \hat{x} - \Delta\hat{x}, \quad \hat{\hat{y}} = \hat{y} - \Delta\hat{y}. \tag{19}$$

This allows one to recalculate X and Y from

$$Y = \tilde{B}_i - \hat{\hat{B}}_i, \quad \hat{\hat{m}}_i = \hat{\hat{y}} - y_1, \quad \text{and} \quad \hat{\hat{n}}_i = \hat{\hat{x}} - x_1. \tag{20}$$

This process can be repeated until some measure of convergence is satisfied. Random errors in the measurements generally cause the process to converge on a point which is not the true emitter position but is on the average the best estimate achievable with the assumptions made.

Up to this point, emitter motion has not been considered; however, the technique can be expanded to consider moving emitters by hypothesizing an "average" position of the emitter during the time interval in which N measurements are taken. This is the approach which has been applied to moving emitters. In essence a statistical moving average of the emitter's position is determined. Initially a rough estimate is made for the $(N + 1)/2$ position based on N measurements made from two remote sites, and this is used in the algorithm as outlined for the stationary emitter. After the algorithm has converged to a "better" estimate, a new measurement is taken, and the oldest of the previous N measurements is discarded. The process is then repeated, and the time series of "better" estimates is used to constitute a track.

A computer model of the process has been developed, and some preliminary results are available. Figure 2 shows the range and crossrange tracking, errors for an emitter approaching site 2 at a speed of 500 units/s. The sites are separated by 20K units, and measurements are made at alternate sites every 2 s. The results shown in Fig. 2 were generated with $N = 7$ and four iterations. Improved tracking performance was obtained by setting $N = 15$. This result is shown in Fig. 3; however, the price paid to achieve this performance is an increase in the time required for track initiation.

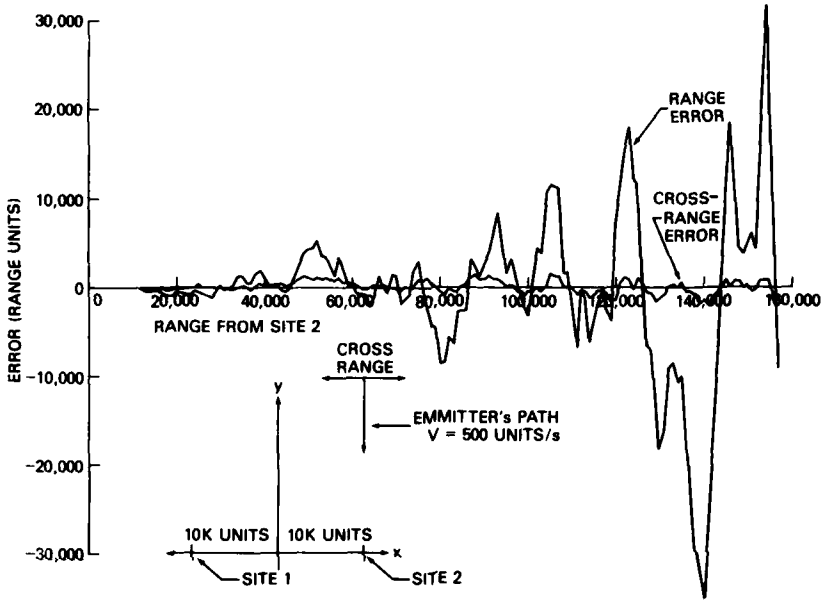

Fig. 2 — Range and crossrange error for $N = 7$ measurements when the statistical moving average technique is used

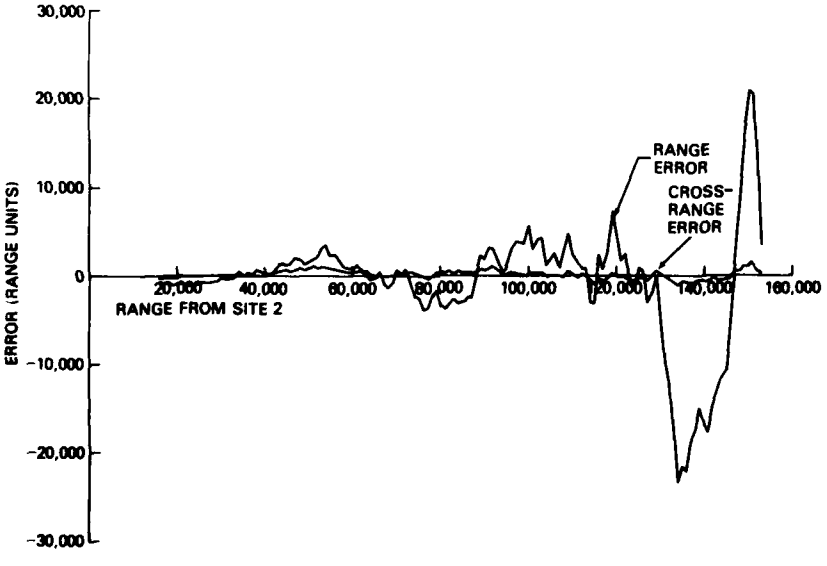

Fig. 3 — Range and crossrange error for $N = 15$ measurements when the statistical moving average technique is used

Suggested in Ref. 1 is that the relative speed of the target with respect to the observer might also affect the performance. When two sites are located as described and alternate readings are made every 2 s, an effective observer speed of ±10K units/s is achieved. To investigate the effect of emitter speed on tracking performance, a scenario was designed with an emitter moving parallel to the baseline. The spacing between the emitter path and the baseline was set at 30K units.

Figures 4 and 5 plot the errors in the x and y coordinates of the emitter's position for emitter speeds of 250 and 1000 units/s respectively. Contrary to the results shown in Ref. 1, tracking performance does not change appreciably for the two speeds considered. This is because with two observers the triangulation effect is not significantly diminished by the motion of the emitter if the distance the emitter moves between measurements is small with respect to the length of the baseline. (For 1000 units/s and a baseline of 20K units the emitter moves 1/10 the length of the baseline every 2 s.) The track for the fast emitter settles down sooner than that of the slow emitter. This is because the fast emitter moves over a greater distance in the measurement interval; consequently some of the measurements of the fast emitter are made at more accurate locations than all of the measurements of the slow emitter.

MODIFIED KALMAN FILTER TECHNIQUE

The second technique to be considered is referred to as the modified Kalman filter technique. Under this technique one of the sites is designated as the reporting site and the other as the updating site. As shown in Fig. 6, the measurements $\gamma(k+1)$ from the reporting site are averaged to produce $\beta_2(k)$. (Since the measurements are equally spaced in time, $\beta_2(k)$ is coincident with $\beta_1(k)$. If the measurements were not equally spaced, a linear

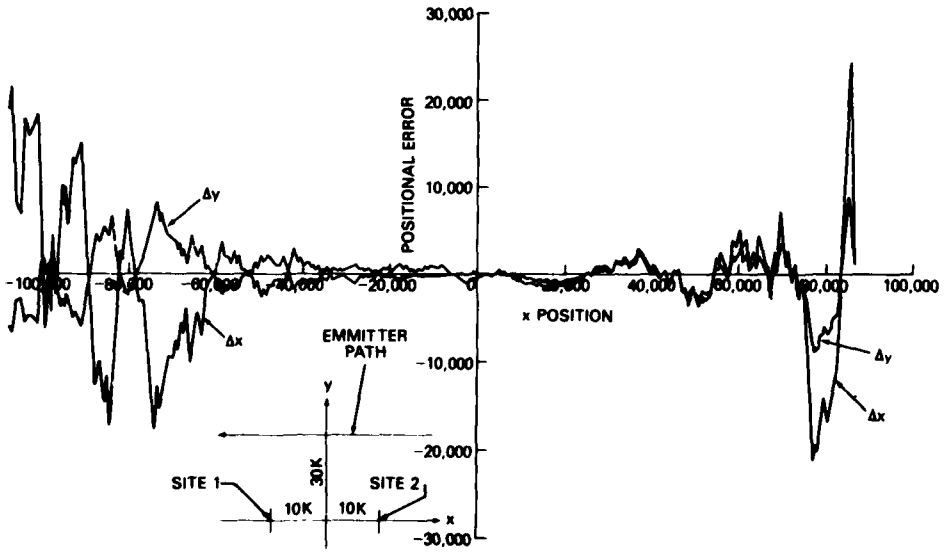

Fig. 4 — Positional error in the x and y coordinates for a crossing emitter with V = 250 units/s when the statistical moving average technique is used

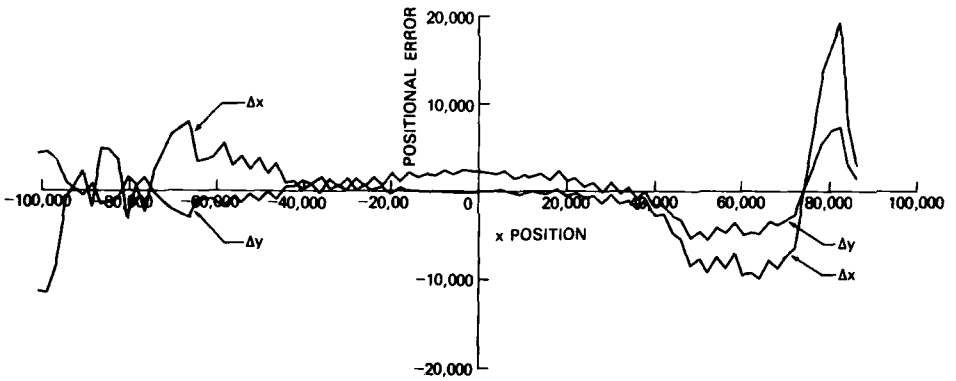

Fig. 5 — Positional error in the x and y coordinates for a crossing emitter with $V = 1000$ units/s when the statistical moving average technique is used

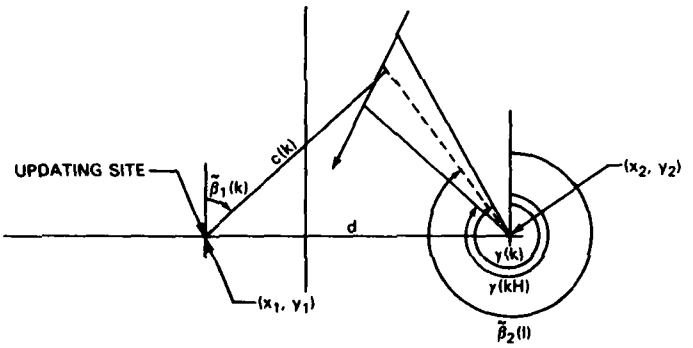

Fig. 6 — Geometry for the modified Kalman filter

interpolation procedure could be employed to make $\beta_2(k)$ coincident with $\beta_1(k)$.) $\beta_2(k)$ and $\beta_1(k)$ are then used to triangulate the position of the emitter, and the coordinates of the emitter are fed into a Kalman filter, which is a tracking algorithm that minimizes the least-square error [5]. The coordinates of the emitter corresponding to the kth measurement by the updating site are given by

$$\tilde{x}(k) = c(k) \sin \beta_1(k) + x_1 , \quad \tilde{y}(k) = c(k) \cos \beta_1(k) + y_1 , \tag{21}$$

where

$$c(k) = d \cos \beta_2(k) / [\sin (\beta_1(k) - \beta_2(k))] .$$

The state equation for the Kalman filter is

$$X(k+1) = \Phi(k) X(k) + \Gamma(k) A(k) , \tag{22}$$

where

$$X(k) = \begin{bmatrix} x(k) \\ \dot{x}(k) \\ y(k) \\ \dot{y}(k) \end{bmatrix}, \quad \Phi(k) = \begin{bmatrix} 1 & T & 0 & 0 \\ 0 & 1 & 0 & 0 \\ 0 & 0 & 1 & T \\ 0 & 0 & 0 & 1 \end{bmatrix}, \quad \Gamma(k) = \begin{bmatrix} \frac{T^2}{2} & 0 \\ T & 0 \\ 0 & \frac{T^2}{2} \\ 0 & T \end{bmatrix}, \quad \text{and} \quad A(k) = \begin{bmatrix} a_x(k) \\ a_y(k) \end{bmatrix},$$

with $X(k)$ being the state vector at time sample k consisting of position and velocity components $x(k)$, $\dot{x}(k)$, $y(k)$, and $\dot{y}(k)$, $k+1$ being the next update time, T being the time between updates, and $a_x(k)$ and $a_y(k)$ being random accelerations whose covariance matrix is $Q(k)$. The observation equation is

$$Y(k) = M(k)X(k) + V(k),$$

where

$$Y(k) = \begin{bmatrix} \tilde{x}(k) \\ \tilde{y}(k) \end{bmatrix}, \quad M(k) = \begin{bmatrix} 1 & 0 & 0 & 0 \\ 0 & 0 & 1 & 0 \end{bmatrix}, \quad \text{and} \quad V(k) = \begin{bmatrix} v_x(k) \\ v_y(k) \end{bmatrix},$$

with $Y(k)$ being the measurement at time sample k consisting of measured positions $\tilde{x}(k)$ and $\tilde{y}(k)$ and with $V(k)$ being zero mean noise whose covariance matrix is $R(k)$.

Any two successive measurements are not strictly independent, due to the overlap of measurements from the reporting site in the triangulation process. Furthermore a bias can be introduced by using an arithmetic average in determining $\beta_2(k)$; however, these inconsistencies do not seem to affect the tracking performance of the algorithm, and these deficiencies can be removed if deemed necessary.

The recursive algorithm which constitutes the filter is described in Ref. 5. The elements of the covariance matrix

$$R(k) = \begin{vmatrix} \sigma_x^2(k) & \sigma_{xy}(k) \\ \sigma_{xy}(k) & \sigma_y^2(k) \end{vmatrix} \tag{23}$$

as derived from Eqs. (21) are (as shown in the Appendix)

$$\sigma_x^2 = \left[d/\sin^2(\beta_1 - \beta_2)\right]^2 \left[\sin^2\beta_1 (\cos^2\beta_1)\sigma_{\beta_2}^2 + \sin^2\beta_2 (\cos^2\beta_2)\sigma_{\beta_1}^2\right], \tag{24}$$

$$\sigma_y^2 = \left[d/\sin^2(\beta_1 - \beta_2)\right]^2 \left[(\cos^4\beta_1)\sigma_{\beta_2}^2 + (\cos^4\beta_2)\sigma_{\beta_1}^2\right], \tag{25}$$

and

$$\sigma_{xy} = \left[d/\sin^2(\beta_1 - \beta_2)\right]^2 \left[\cos^3\beta_1 (\sin\beta_1)\sigma_{\beta_2}^2 + \cos^3\beta_2 (\sin\beta_2)\sigma_{\beta_1}^2\right], \tag{26}$$

where the kth-sample notation is not shown.

The performance of this algorithm was examined using the same scenarios used in the previous examples. Figure 7 shows the range and crossrange error for an emitter approaching site 2, and Figs. 8 and 9 give the errors in the emitter's x and y coordinates for an emitter flying parallel to the baseline at speeds of 250 and 1000 units/s. For both the radial and crossing emitters the modified Kalman filter gives a significantly better track than that developed by the moving average technique.

EXTENDED KALMAN FILTER TECHNIQUE

The third technique to be considered is described in Refs. 2 and 3. In these studies primary consideration was given to the special case in which all the bearing measurements were made by a single moving platform. As described subsequently, the technique has been applied to the multisite case with two or more sites making asynchronous observations of a moving emitter.

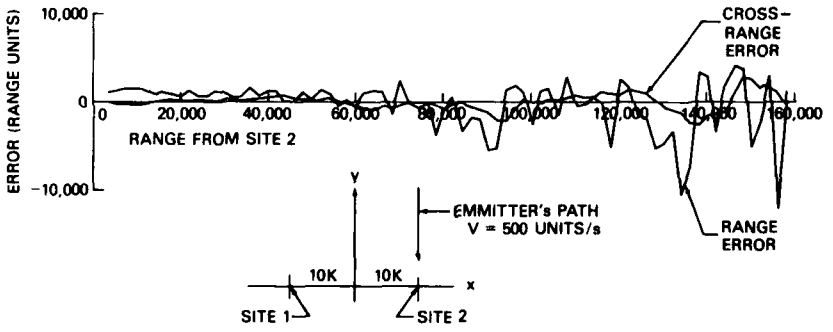

Fig. 7 — Range and crossrange error when the modified Kalman filter is used

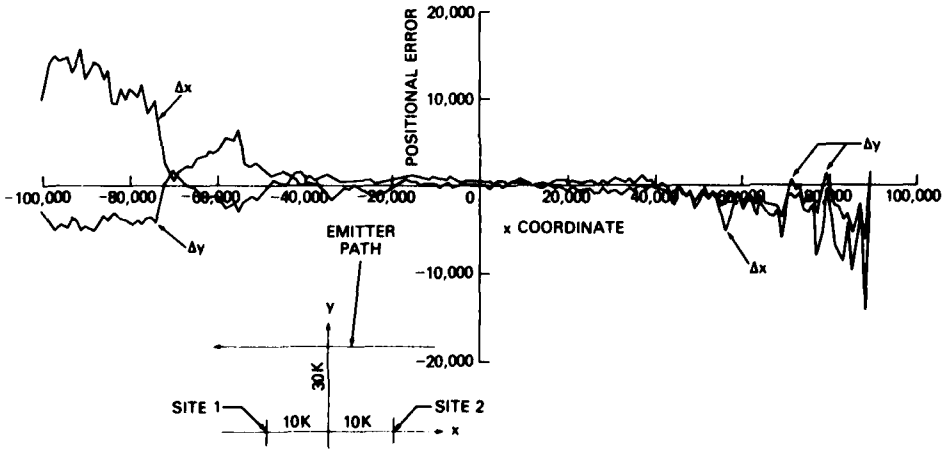

Fig. 8 — Positional error in the x and y coordinates for a crossing emitter with V = 250 units/s when the modified Kalman filter is used

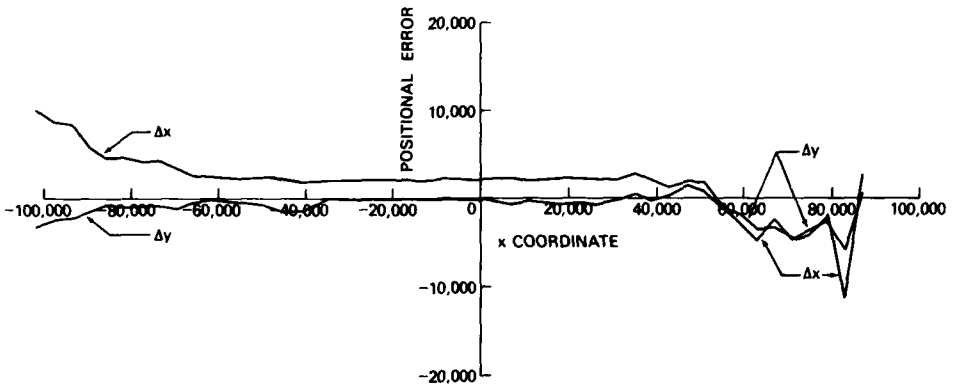

Fig. 9 — Positional error in the x and y coordinates for a crossing emitter with V = 1000 units/s when the modified Kalman filter is used

The geometry of the situation is shown in Fig. 10. For observation k the bearing measurement $\beta(k)$ assuming no noise is given by

$$\tan \beta(k) = [x_T(k) - x_i]/[y_T(k) - y_i] , \tag{27}$$

where the target location is given by the coordinates $x_T(k)$ and $y_T(k)$ and the ith site location is given by the coordinates x_i and y_i. Equivalently (27) can be written as

$$[x_T(k) - x_i] \cos \beta(k) - [y_T(k) - y_i] \sin \beta(k) = 0 . \tag{28}$$

Further manipulation yields

$$x_i \cos \beta(k) - y_i \sin \beta(k) = x_T(k) \cos \beta(k) - y_T(k) \sin \beta(k) . \tag{29}$$

If the left-hand side of (29) is considered as a measurement, it can be rewritten as

$$x_i \cos \tilde{\beta}(k) - y_i \sin \tilde{\beta}(k) = x_T(k) \cos \beta(k) - y_T(k) \sin \beta(k) + N , \tag{30}$$

where $\tilde{\beta}(k)$ is the kth bearing measurement corrupted by noise and N represents the noise in the measurement process. Equation (30) can be rewritten in the form of an observation equation for the Kalman filter:

$$Z(k) = M(k)X_T(k) + N(k) , \tag{31}$$

where

$$Z(k) = x_i \cos \tilde{\beta}(k) - y_i \sin \tilde{\beta}(k) ,$$

$$X_T(k) = \begin{bmatrix} x_T \\ y_T \\ \dot{x}_T \\ \dot{y}_T \end{bmatrix} ,$$

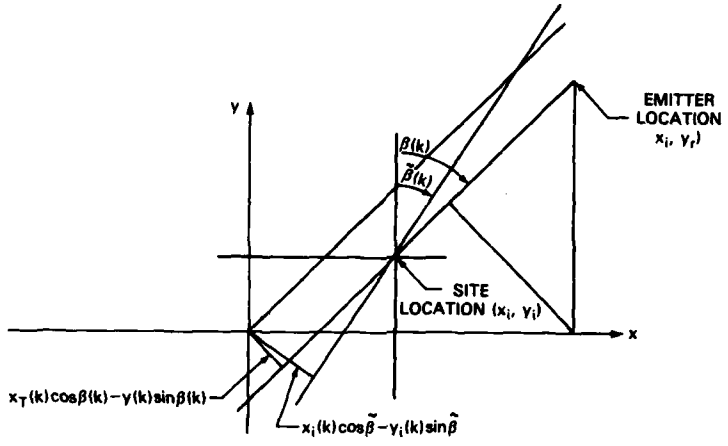

Fig. 10 — Geometry for the extended Kalman filter

and

$$M(k) = [\cos\beta(k), -\sin\beta(k), 0, 0].$$

The corresponding state equation, which was described in Ref. 5, together with the observation equation are in a form resembling that of a linear estimation problem. Despite the nonlinearities in the observation equation an attempt was made to apply linear estimation techniques. Before this was done, two approximations were made: the matrix $M(k)$ was replaced by

$$\tilde{M}(k) = [\cos\tilde{\beta}(k), -\sin\tilde{\beta}(k), 0, 0], \tag{32}$$

and the variance of $N(k)$, denoted by $\sigma_N^2(k)$, was approximated by (as derived in the Appendix)

$$\sigma_N^2(k) = \left(x_i^2\sigma_\beta^2 + \sigma_{y_i}^2\right)\sin^2\tilde{\beta} + \left(\sigma_{x_i}^2 + y_\beta^2\right)\cos^2\tilde{\beta} - 2\sin\tilde{\beta}\,(\cos\tilde{\beta})x_i y_i\sigma_\beta^2, \tag{33}$$

where $\sigma_{x_i}^2$ and $\sigma_{y_i}^2$ are the error variances in the location of the observation sites and σ_β^2 is the variance in the bearing measurement.

The measurement $Z(k)$ is essentially the perpendicular distance from the origin to the bearing line (Fig. 10), and this distance depends on the location of the sites with respect to the origin. Because of this feature it was advantageous to locate both receiving sites on one of the coordinate axis. For sites on the x axis $y_i = 0$, and the variance (33) is reduced to

$$\sigma_N^2(k) = \left(x_i^2\sigma_\beta^2 + \sigma_{y_i}^2\right)\sin^2\tilde{\beta} + \sigma_{x_i}^2\cos^2\tilde{\beta}. \tag{34}$$

With these assumptions the algorithm described in Ref. 2 was exercised, with results as follows.

The same scenarios which were described in the two previous sections were used to examine the performance of the algorithm. Figure 11 shows the range and crossrange errors for an emitter approaching site 2 at a speed of 500 units/s. It was assumed for all of the scenarios that the locations of both sites were known almost exactly; that is, $\sigma_{x_i} = \sigma_{y_i} = 10$ units, and a value $\sigma_\beta = 1^\circ$ was used in computing the errors. Figures 12 and 13 show the errors in the emitter's x and y coordinates for an emitter flying parallel to the baseline at speed of 250 and 1000 units/s respectively. In general the extended Kalman filter takes longer to settle down than the modified Kalman filter; however, the track for the slow emitter, moving parallel to the baseline, is more accurate once it is fully developed.

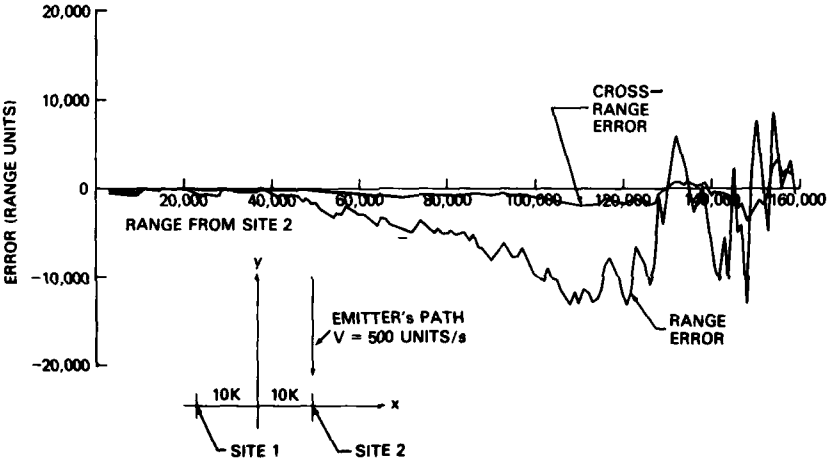

Fig. 11 — Range and crossrange error when the extended Kalman filter is used

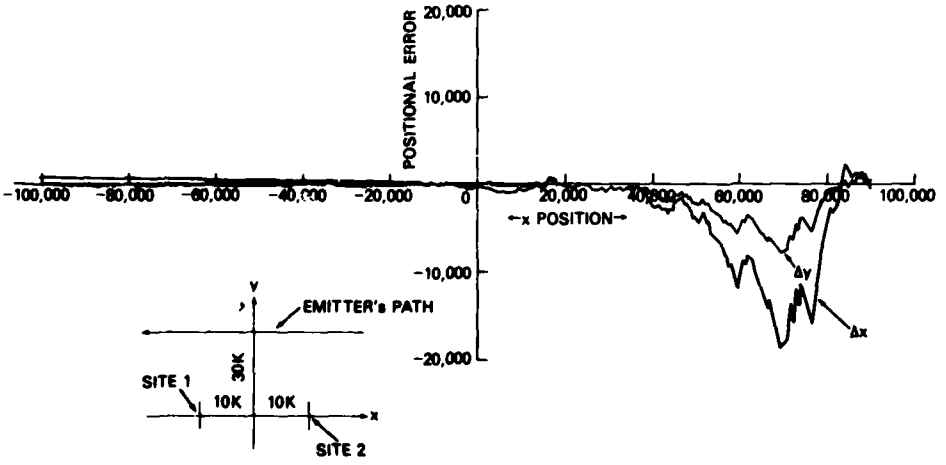

Fig. 12 — Positional error in the x and y coordinates for a crossing emitter with $V = 250$ units/s when the extended Kalman filter is used

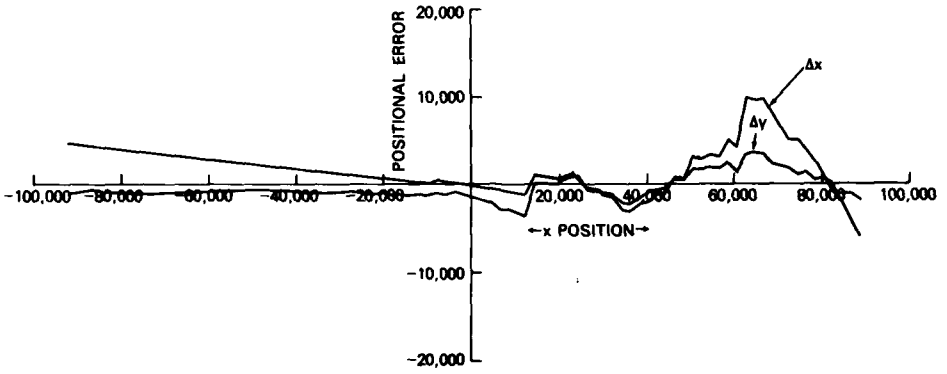

Fig. 13 — Positional error in the x and y coordinates for a crossing emitter with V = 1000 units/s when the extended Kalman filter is used

SUMMARY

Three algorithms have been developed which use bearing measurements from two remote sites to track moving emitters. Preliminary results indicate that the modified Kalman filter technique is superior to the other two techniques in its ability to rapidly develop a reasonable track. The extended Kalman filter demonstrated superior tracking performance once it had settled down; however, for the cases considered this required an unreasonable amount of time. Further investigation is required to assess the performance of the algorithms against maneuvering targets. The effect of varying the time between measurements should also be considered.

REFERENCES

1. J. L. Poirot and M. S. Smith, "Moving Emitter Classification," IEEE Transactions on Aerospace and Electronic Systems AES-12 (No. 2), 255-269 (Mar. 1976).
2. A. G. Lindgren and K. F. Gong, "Position and Velocity Estimation Via Bearing Observation," IEEE Transactions on Aerospace and Electronic Systems AES-14 (No. 4), 564-577 (July 1978).
3. V. J. Aidala, "Kalman Filter Behavior in Bearings-Only Tracking Applications," IEEE Transactions on Aerospace and Electronic Systems AES-15 (No. 1), 29-39 (Jan. 1979).
4. F. A. Graybill, *An Introduction to Linear Statistical Models*, New York, McGraw-Hill, 1961.
5. G. V. Trunk and J. D. Wilson, "Tracking Filters for Multiple-Platform Radar Integration," NRL Report 8087, Dec. 1976.

Appendix
DERIVATIONS OF EQUATIONS (24) AND (33)

DERIVATION OF EQ. (24)

From Eq. (21)

$$x(k) = c \sin \beta_1 + x_1$$

$$= d \cos \beta_2 \sin \beta_1 / [\sin (\beta_1 - \beta_2)] .$$

The differential form of $x(k)$ is

$$\Delta x = d [-\sin \beta_2 \sin \beta_1 / \sin (\beta_1 - \beta_2) + \cos \beta_2 \sin \beta_1 \cos (\beta_1 - \beta_2) / \sin^2 (\beta_1 - \beta_2)] \Delta \beta_2$$

$$+ d [\cos \beta_1 \cos \beta_2 / \sin (\beta_1 - \beta_2) - \cos \beta_2 \sin \beta_1 \cos (\beta_1 - \beta_2) / \sin^2 (\beta_1 - \beta_2)] \Delta \beta_1 .$$

Using trigonometric substitutions and combining terms yields

$$\Delta x = d [\sin \beta_1 \cos \beta_1 / \sin^2 (\beta_1 - \beta_2)] \Delta \beta_2 - d [\sin \beta_2 \cos \beta_2 / \sin^2 (\beta_1 - \beta_2)] \Delta \beta_1 .$$

Since $E(\Delta x) = E(\Delta \beta_1) = E(\Delta \beta_2) = 0$

$$\text{and } \sigma_x^2 = E(\Delta x^2), \ \sigma_{\beta_1} = E(\Delta \beta_1), \text{ and } \sigma_{\beta_2} = E(\Delta \beta_2),$$

the result is

$$\sigma_x^2 = [d / \sin^2 (\beta_1 - \beta_2)]^2 \left[\sin^2 \beta_1 \left(\cos^2 \beta_1 \, \sigma_{\beta_2} \right) + \sin^2 \beta_2 \left(\cos^2 \beta_2 \right) \sigma_{\beta_1}^2 \right] .$$

Equations (25) and (26) are derived similarly.

DERIVATION OF EQ. (33)

The measurement Z_m can be expressed as

$$Z_m = Z + \Delta Z ,$$

where

$$\Delta Z = (\partial Z / \partial x_i) \Delta x_i + (\partial Z / \partial y_i) \Delta y_i + (\partial Z / \partial_\beta) \Delta \beta$$

$$= (\cos \beta)(\Delta x_i - y_i \Delta \beta) - (\sin \beta)(x_i \Delta \beta + \Delta y_i) .$$

The assumption that $\Delta Z \approx N$ gives

$$\sigma_n^2 = \left(x_i^2\sigma_\beta^2 + \sigma_{y_i}^2\right)\sin^2\tilde{\beta} + \left(\sigma_{x_i}^2 + y_i^2\sigma_\beta^2\right)\cos^2\tilde{\beta}$$

$$-2\sin\tilde{\beta}\,(\cos\tilde{\beta})x_i y_i \sigma_\beta^2 .$$